STABILITY OF FLEXURAL CRACKS IN PARTIALLY PRESTRESSED CONCRETE I-BEAMS

PRAKASH DESAYI*

(*Department of Civil Engineering, University of Leeds, Leeds LS2 9JT, U.K.*)

Received on July 17, 1976

ABSTRACT

Assuming non-linear stress-blocks for concrete in compression and tension, variation of resisting moment of a prestressed concrete beam of I-section has been studied with the gradual penetration of a flexural crack. The range of instability of the crack is examined with respect to the effective prestrain, area of tensioned and non-tensioned reinforcement and the bonding efficiency. For an illustrative case, the minimum reinforcement for a stable crack is determined.

Key words: Beams (structural); Bonding efficiency; Concrete (partially prestressed); Cracks (flexural); Effective prestrain; Reinforcement (non-tensioned); Stability.

INTRODUCTION

In class 3 prestressed concrete structures [1], cracking is permitted and such beams are also normally reinforced with non-tensioned steel. Recently, considerable attention is being paid to a study of the cracking characteristics of such beams so as to develop suitable methods of examining them for the limit state of cracking. Whilst many studies have aimed at a determination of the widths of cracks developed in prestressed and reinforced concrete members, the unstable behaviour of a flexural crack has been studied only by a few investigators. During testing a reinforced, prestressed or partially prestressed concrete beam, just at cracking, it is noticed that sometimes a flexural crack suddenly extends to a considerable height accompanied by a sudden drop in the load. Subsequently the crack penetrates further with or without increase in loading depending on the amount of reinforcement—thus the crack shows an initial unstable behaviour just when it forms and

* Present address: Department of Civil Engineering, Indian Institute of Science, Bangalore 560012, India.

subsequently remains unstable or becomes stable. The unstable cracking behaviour is important for the reason that, in relation to the load carrying capacity, a stable crack is compatible with additional load carrying capacity while unstable cracking leads to failure. Also, if the crack is unstable over a considerable height, the cracks would be wider and spaced farther apart—a situation which is undesirable and which is to be avoided.

Krahl, Khachaturian and Siess [2] appear to be the first to study the stability of tensile cracks in concrete beams. They found that in a plain concrete beam the crack is unstable from the stage of inception till failure and that addition of reinforcement stabilizes the crack. The method was also used to study the stability of tensile cracks, if they form at the top fibre of a prestressed concrete beam at transfer of prestress. Oladapo [3] studied the stability of flexural cracks in prestressed beams and noticed that the range of instability was reduced by a higher level of prestress. Also, increase in the steel ratio stabilised the cracks at all stages. In both the above studies, the resisting moment of the cross-section was determined by assuming an elastic-plastic behaviour for concrete in compression and elastic behaviour in tension and by taking bond factor for steel to be unity. Beeby [4, 5] determined the initial crack height (corresponding to the unstable height of the flexural crack) of reinforced concrete beams of rectangular and T-sections in connection with the determination of crack widths. For determining the resisting moment, he assumed a triangular stress-block for compression and tension in concrete.

Noting that the stress-strain plots of concrete in compression and tension are curved, and can as such be taken to represent the stress-blocks instead of approximating them to be triangular or trapezoidal, and investigation was undertaken to study the stability of flexural cracks of prestressed concrete beams with curved stress-blocks for compression and tension of concrete. The analysis covered the cases of beams of I-section and the bonding efficiency of prestress steel and non-tensioned steel. This paper presents briefly some of the results which have been reported in greater detail elsewhere [6].

ANALYSIS

Stability of a flexural crack is examined by finding how the resisting moment varies with the progress of the crack into the beam. For this purpose, the resisting moment of the cross-section of an I-beam having prestress steel and non-tensioned steel is determined as the crack forms and penetrates into the section. Upto the stage of decompression, the elastic analysis is fairly applicable for the prestressed beam section and hence it would be sufficient if the analysis with the curved stress-blocks is applied for the situation after the decompression of bottom fibre. The resisting moment at the stage of decompression depends on the degree of prestress and can be determined for the gross transformed section and hence is not included in the analysis. The present analysis therefore determines the moment in excess of that decompression stage, *i.e.*, M_e. The total resisting moment M, at any stage can be obtained from $M = M_e + M_{de}$ where M_{de} is the moment corresponding to the stage of decompression. The analysis is first presented and followed by the numerical results of a case worked out for illustration.

The method of force equilibrium and strain compatiblity is used to find the resisting moment and curvature. Along with the usual assumptions that plane sections remain plane and the cross-section is subjected to pure flexure, it is assumed that concrete cracks on reaching a limiting tensile strain.

The equation for the stress-strain curve of concrete in compression (Fig. 1 *a*) is taken to be [7],

$$f_c = \frac{2 f_{oc} \epsilon_c / \epsilon_{oc}}{1 + \left(\frac{\epsilon_c}{\epsilon_{oc}}\right)^2} \tag{1}$$

If f_{ac} is the average stress of the shaded portion and ϵ_c is the strain at the centroid of the area, then

$$f_{ac} = \alpha_c f_{oc} \tag{2 a}$$

with

$$\alpha_c = \frac{\epsilon_{oc}}{\epsilon_c} \log_e \left[1 + \left(\frac{\epsilon_c}{\epsilon_{oc}}\right)^2\right] \tag{2 b}$$

and

$$\epsilon_{cc} = \beta_c \epsilon_c \tag{3 a}$$

with

$$\beta_c = \frac{2\left[1 - \frac{\epsilon_{oc}}{\epsilon_c} \tan^{-1} \frac{\epsilon_c}{\epsilon_{oc}}\right]}{\log_e\left[1 + \left(\frac{\epsilon_c}{\epsilon_{oc}}\right)^2\right]} \tag{3 b}$$

Referring to the shaded area in Fig. 1 *b*, which is between the ordinates ϵ_{c1} and ϵ_{c2}, if f_{c12} is the average stress in this area and if $\bar{\epsilon}_{c12}$ is the strain at the centroid of this area, then

$$f_{c12} = f_{oc}\, \alpha_{c12} \tag{4 a}$$

with

$$\alpha_{c12} = \frac{\epsilon_{oc}}{\epsilon_{c2} - \epsilon_{c1}} \log_e \left[\frac{1 + \left(\frac{\epsilon_{c2}}{\epsilon_{oc}}\right)^2}{1 + \left(\frac{\epsilon_{c1}}{\epsilon_{oc}}\right)^2}\right] \tag{4 b}$$

and

$$\bar{\epsilon}_{c12} = \beta_{c12}\, \epsilon_{c2} \tag{5 a}$$

with

$$\beta_{c12} = \frac{2\left[1 - \frac{\epsilon_{oc}}{\epsilon_{c2}} \tan^{-1} \frac{\epsilon_{c2}}{\epsilon_{oc}}\right] - 2\left[\frac{\epsilon_{c1}}{\epsilon_{c2}} - \frac{\epsilon_{oc}}{\epsilon_{c2}} \tan^{-1} \frac{\epsilon_{c1}}{\epsilon_{oc}}\right]}{\log_e \left[\frac{1 + \left(\frac{\epsilon_{c2}}{\epsilon_{oc}}\right)^2}{1 + \left(\frac{\epsilon_{c1}}{\epsilon_{oc}}\right)^2}\right]} \tag{5 b}$$

The stress-strain curve of concrete in tension (Fig. 2) is assumed to be of a form similar to that in compression and its equation taken to be

$$f_t = \frac{2 f_{ot} \frac{\epsilon_t}{\epsilon_{ot}}}{1 + \left(\frac{\epsilon_t}{\epsilon_{ot}}\right)^2} \tag{6}$$

For full or part areas under the tensile stress-strain curve, relations similar to those of equations (2 *a*) to (5 *b*) can be written down with ϵ_t, ϵ_{ot}, f_{at}, f_{ot}, α_t, β_t, f_{t12}, α_{t12}, ϵ_{t2}, ϵ_{t1}, β_{t12} replacing the corresponding quantities of the compression case. Thus α_t, β_t, α_{t12} and β_{t12} are known.

The stress-strain curve of the prestressing steel is approximated to the bilinear form as shown in Fig. 3. The two straight lines are then represented by:

for

$$\epsilon_s \leqslant \epsilon_{sy}, f_s = E_{s1}\, \epsilon_s \tag{7 a}$$

and for

$$\epsilon_{sy} \leqslant \epsilon_s \leqslant \epsilon_{su}, f_s = f_{sy} + E_{s2}(\epsilon_s - \epsilon_{sy}) \tag{7 b}$$

where

$$E_{s1} = \frac{f_{sy}}{\epsilon_{sy}}$$

and

$$E_{s2} = \frac{f_{su} - f_{sy}}{\epsilon_{su} - \epsilon_{sy}} \tag{7 c}$$

The stress-strain curve of non-tensioned steel is assumed to be elastic-plastic (Fig. 4) and so,

for

$$\epsilon_{sn} \leqslant \epsilon_{syn}, f_{sn} = E_{sn}\, \epsilon_{sn} \tag{8 a}$$

and for

$$\epsilon_{sn} > \epsilon_{syn}, f_{sn} = f_{sy} \tag{8 b}$$

where

$$E_{sn} = f_{syn}/\epsilon_{syn}, \tag{8 c}$$

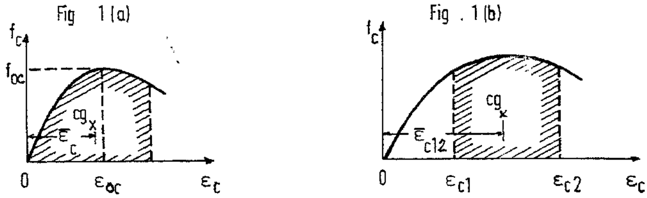

Fig . 1 . Stress–strain curve of concrete in compression

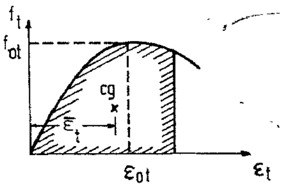

Fig . 2 . Stress–strain curve of concrete in tension

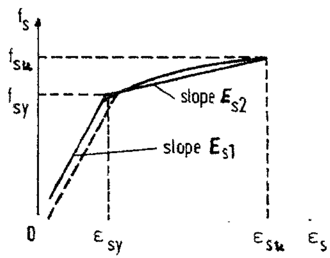

Fig . 3 . Stress–strain curve of prestress steel and the bilinear approximation

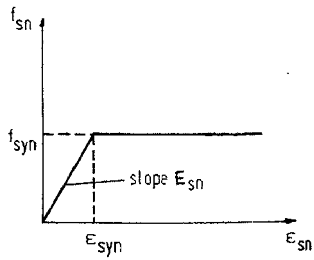

Fig . 4 . Stress-strain curve of non-tensioned steel

When the prestressed concrete beam section (Fig. 5) is subjected to a moment M_e, depending on the closeness of $M_c + M_{de}$ to ultimate moment the following cases arise: (*a*) tip of the crack being in the bottom flange with neutral axis in the web, (*b*) tip of crack and neutral axis are in the web, (*c*) tip of crack is in the web and the neutral axis in the top flange and (*d*) tip of crack and neutral axis are in the top flange. While studying the crack stability it might be sufficient to examine the first two cases as the cases (*c*) and (*d*) arise mostly for moments close to the ultimate moment. Instability of the crack, if any, would be revealed while analysing for cases (*a*) and (*b*).

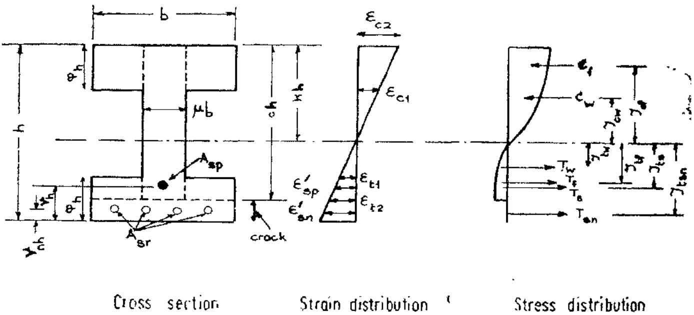

Fig. 5. Strain and stress distributions (case 1)

Case 1: Tip of crack in the bottom flange and neutral axis in the web: Figure 5 shows the strain and stress distuibution across the cross-section. The position of neutral axis can be got from the condition,

$$C_f + C_w = T_f + T_w + T_s + T_{sn} \tag{9}$$

and the resisting moment is given by,

$$M_e = C_f\, y_{cf} + C_w y_{cw} + T_f y_{tf} + T_w y_{tf} + T_s y_{ts} + T_{sn} y_{sn}. \tag{10}$$

The curvature may then be obtained from

$$\chi_e = \epsilon_{c2}/kh, \tag{11}$$

The various compressive and tensile forces and their location can be derived as the following:

$$C_f = (1 - \mu)\, \phi\, \alpha_{c12}\, bhf_{oc} \tag{12}$$

and

$$y_{cf} = \beta_{c12} kh \tag{13}$$

where α_{c12}, β_{c12} are given by equations (4 *b*) and (5 *b*) and with

$$\epsilon_{c2} = \frac{k}{c - k}\, \epsilon_{t2} \tag{14 a}$$

and

$$\epsilon_{c1} = \frac{k - \phi}{c - k}\, \epsilon_{t2} \tag{14 b}$$

$$C_w = \mu k \alpha_c\, bh\, f_{oc} \tag{15}$$

and

$$y_{cw} = \beta_c\, kh \tag{16}$$

where α_c and β_c are given by equations (2 *b*) and (3 *b*) with $\epsilon_c = \epsilon_{c2}$ (=eq. 14 *a*).

$$T_f = (1 - \mu)\,(c + \phi - 1)\, \alpha_{t12}\, bhf_{ot} \tag{17}$$

and

$$y_{tf} = \beta_{t12}\,(c - k)\, h \tag{18}$$

with

$$\epsilon_{t1} = \frac{(1 - \phi - k)}{(c - k)}\, \epsilon_{t2} \tag{19}$$

$$T_w = \mu\,(c - k)\, \alpha_t\, bhf_{ot} \tag{20}$$

and

$$y_{tw} = \beta_t\,(c - k)\, h \tag{21}$$

Tension in the prestress steel depends on the magnitude of the strain $(\epsilon_{sp} + \theta_p\, \epsilon'_{sp})$ where θ_p is the bond factor and two cases arise:
If

$$(\epsilon_{sp} + \theta\epsilon'_{sp}) \leqslant \epsilon_{sy}$$
$$T_s = (\epsilon_{sp} + \theta_p\, \epsilon'_{sp})\, E_{s1}\, A_{sp} \tag{22}$$

or, if

$$\epsilon_{sy} < (\epsilon_{sp} + \theta_p\, \epsilon'_{sp}) \leqslant \epsilon_{su},$$
$$T_s = [\,\epsilon_{sy}\, E_{s1} + (\epsilon_{sp} + \theta_p\, \epsilon'_{sp} - \epsilon_{sy})\, E_{s2}]\, A_{sp}. \tag{23}$$

In equations (22) and (23),

$$\epsilon'_{sp} = \frac{(1 - r - k)}{(c - k)}\, \epsilon_{t2} \tag{24}$$

and

$$y_{ts} = (1 - r - k)\, h \tag{25}$$

Strain in the non-tensioned steel is $(-\,\epsilon_{sn} + \theta_n\epsilon'_{sn})$ where θ_n is the bond factor and the strain ϵ_{sn} is assumed to be compressive as it would normally be. Again two alternatives arise depending on the level of steel strain:

If

$$(-\,\epsilon_{sn} + \theta_n\, \epsilon'_{sn}) < \epsilon_{syn},$$
$$T_{sn} = (-\,\epsilon_{sn} + \theta_n\, \epsilon'_{sn})\, E_{sn}\, A_{sn} \tag{26}$$

Or, if

$$(-\,\epsilon_{sn} + \theta_n\, \epsilon'_{sn}) \geqslant \epsilon_{syn},$$
$$T_{sn} = f_{syn}\, A_{sn}. \tag{27}$$

In equations (26) and (27),

$$\epsilon'_{sn} = \frac{(1 - r_n - k)}{(c - k)}\, \epsilon_{t2} \tag{28}$$

and

$$y_{tsn} = (1 - r_n - k)\, h \tag{29}$$

While using eq. (9), it might be noted that four possibilities arise depending on the level of strain in the prestressed and non-tensioned steels.

Case 2: Tip of the crack and neutral axis are in the web.: Figure 6 shows the strain and stress distribution across the cross-section. This case leads to equation similar to those of case (1) but with the modification that from the equations of case (1), those corresponding to T_f and $T_f\, y_{tf}$ disappear.

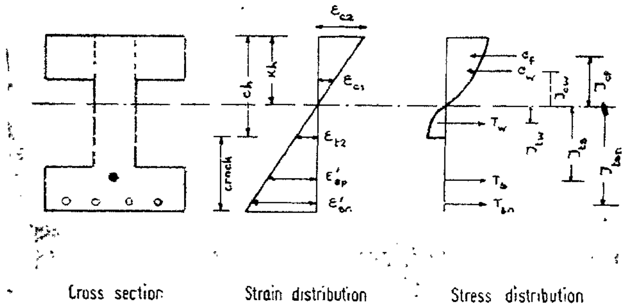

Fig. 6. Strain and stress distributions (case 2)

From the above analysis, M_e and χ_e can be obtained for a given penetration of the crack into the beam and the variation of M_e with the cracked or uncracked depth determined to examine the stability of the crack. In the plots of M_e *versus* ch (uncracked depth), in the region where M_e assumes a value less than its value at $c = 1$, the crack is unstable and it is stable when M_e shows an increase for a decrease in the value of ch.

Illustrative Example

The analysis can be used effectively with a computer to work out numerical results for a given data. One convenient procedure would be to determine M_e and χ_e for a given value of ch. For any assumed value of ch, the position of neutral axis (kd) is to be determined by a trial and error procedure using equation (9). In the process of computation, a value of k requires to be initially assumed and is subsequently altered in suitable steps so that the left hand side and right hand side of equation (9) are equal within reasonable limits. With kd thus known, M_e and χ_e follow. Numerical results are worked out using a ICL 1906A computer for an assumed set of parameters to serve for an illustration and also to give an insight into how moments and curvature change as crack penetrates deeper and deeper into the beam, how the bond factors affect the stability of the crack and what combinations of ϵ_{sp}, ρ_{sp}, ρ_{sn} give a completely stable crack.

The following are the values of various parameters used in the illustration:

Fixed parameters: (*a*) Concrete cube strength $f_{cu} = 5802$ psi (40 N/mm^2). Concrete cylinder strength $f_{oc} = 0{\cdot}8\ f_{cu} = 4642$ psi (32 N/mm^2). For this concrete, from an equation given by Saenz (Discussion of reference [6] $\epsilon_{oc} = 0{\cdot}00192$ (*b*) Tensile strength of this concrete has been obtained after studying the tensile strength obtained by Humphreys [8] and Spetla and Kadlacek [9] as $f_{ot} = 282$ psi (1·95 N/mm^2) (Appendix I). The results of Todd [10] indicate that a value of 10×10^{-5} could be taken for ϵ_{ot} and also for the limiting tensile strain (ϵ_{t2}) of concrete. Evans [11] has reported on the microcracking of concrete in tension at stresses which are about 15 percent to 20 percent less than f_{ot}. This reduced stress could be critical when considering a situation where a concrete beam is subjected to sustained loading with the tensile stress in extreme fibre close to the one at the micro-cracking stage. However, when the concrete is cracked in a short-time test, it appears reasonable to assume that the full stress at f_{ot} is realized and thus a strain of ϵ_{ot} is taken as the limiting tensile strain. (*c*) From tension tests on 0·276 in (7 mm) prestessing wires, the following data wereobtained: $f_{sy} = 174$ kips/in^2 (1200 N/mm^2), $\epsilon_{sy} = 0{\cdot}006$, $f_{su} = 223$ kips/in^2 (1540 N/mm^2), $\epsilon_{su} = 0{\cdot}056$, $E_{s1} = 29 \times 10$ psi (200 KN/mm^2) and $E_{s2} = 0{\cdot}985 \times 10^6$psi (6·8 KN/mm^2). For non-tensioned steels, consisting of high strength deformed bars, $f_{syn} = 59{\cdot}5$ kips/in^2 (410 N/mm^2), $E_{sn} = 29 \times 10^6$ psi (200 KN/mm^2) and $\epsilon_{syn} = 0{\cdot}00205$. (*d*) Covers to the centres of steel bars have been so assumed that $r = 0{\cdot}15$ and $r_n = 0{\cdot}10$. (*e*) The value of ϵ_{sn} is usually very small and is assumed to be zero for convenience.

Variable parameters: (*a*) Flange and Web thicknesses of the cross-section: Two combinations were assumed, *viz.*, $\phi = 0{\cdot}2$, $\mu = 0{\cdot}333$ and $\phi = 0{\cdot}16$, $\mu = 0{\cdot}20$, (*b*) Amount of prestress steel: five values as $\rho_{sp} = 0{\cdot}001$ to $0{\cdot}005$ at $0{\cdot}001$ intervals, (*c*) Prestrain in the prestress steel at the the stage of decompression: five values as $\epsilon_{sp} = 0{\cdot}001$ to $0{\cdot}005$ at $0{\cdot}001$ intervals. (*d*) Non-tensioned steels: five values as $\rho_{sn} = 0{\cdot}0$ to $0{\cdot}02$ at $0{\cdot}005$ intervals (*c*) Bond factors for the two steels: noting that Bennett and

O'keefe [12] suggest bond factors of 1·0 for good bond and 0·4 for poor bond, the following three cases were investigated: $\theta_p = \theta_n = 1 \cdot 0$, $\theta_p = 0 \cdot 4$ and $\theta_n = 1 \cdot 0$, $\theta_p = \theta_n = 0 \cdot 4$. The third case was introduced to find the result of a chance occurrence when both the steels are poorly bonded at a particular section (*f*) Position of the tip of the crack: seven values of c as $c = 1 \cdot 0$ to 0·4 at 0·1 intervals.

RESULTS

(*a*) *Stability of cracks*: Figure. 7 shows typical variation of moment with uncracked depth. Some of the general obsrvations from these plots are as follows: For a given value of ρ_{sp}, and at low values of ϵ_{sp} and ρ_{sn}, the crack is unstable to start with and regains some stability after penetrating to some depth in the tension flange. When the crack reaches the web, because of a sudden decrease of width, it penetrates to larger depths even for small increase in moment. In some cases, the crack may show again an unstable behaviour as it enters the web. For higher values of ϵ_{sp} and/or ρ_{sn}, the instability of the crack in the web first disappears but it still persists in the bottom flange position. Finally for certain combinations of ρ_{sp}, ϵ_{sp} and ρ_{sn}, the cracks show a stable behaviour right from the stage of inception.

(*b*) *Influence of bond factors and effective prestrain*: Fig. 8 shows a typical plot of M_e *versus* c indicating how the bond factor and effective prestrain influence the stability of crack and the magnitude of M_e. As is expected, with a poor bond and for smaller ϵ_{sp}-values, M_e is less for a given depth of crack. When the bond is poor, for a given ρ_{sp}, a higher ϵ_{sp} is needed to make the crack stable in the tension flange. Figure 9 shows a typical plot of how the curvature χ_e changes with incrasing crack depth. In the region where the crack is unstable, it is only the moment that decreases whereas deformations are on the increase. A kink noticed at $c = 0 \cdot 8$ in all curves corresponds to the position of crack at the junction of the flange and web. For higher values of effective prestrain, higher curvature is obtained for a given crack depth; for a given ϵ_{sp}, poorer bond leads to smaller curvatures. Figure. 10 shows typical plots of the variation of moment with curvature and how effective prestrain and bond factors influence the same. The section is stiffer and stronger with higher prestrain and better bond.

(*c*) *Influence of cross-sectional parameters*: From the two alternate combinations of ϕ and μ for which the computations were made, the section with thinner web and flange required higher values of ϵ_{sp}, ρ_{sp} and ρ_{sn} to keep the crack stable over its centire range of formation,

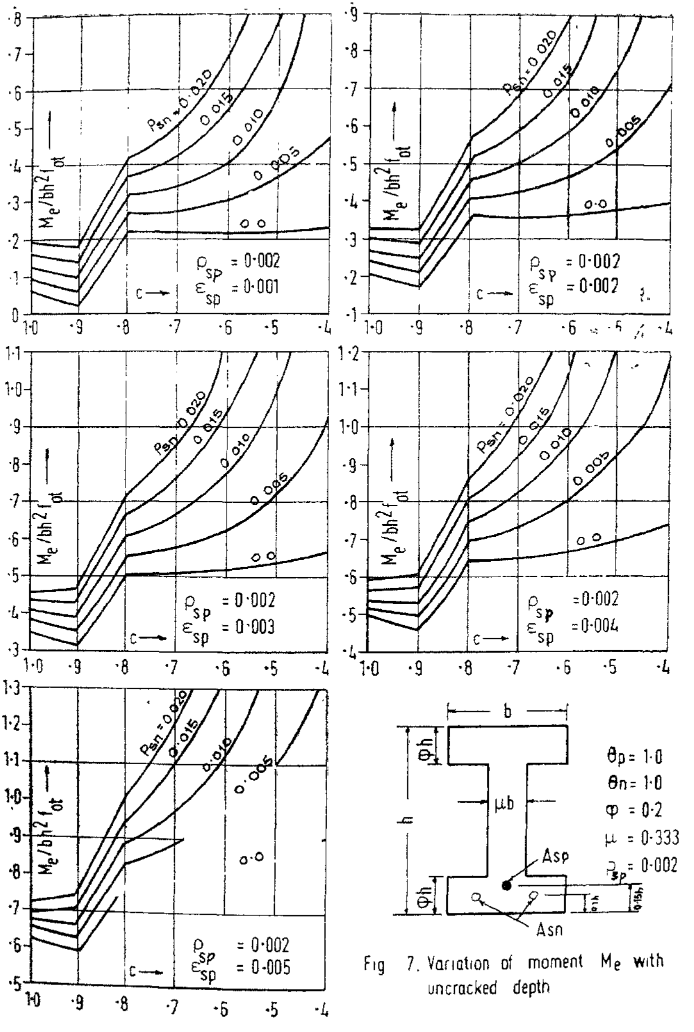

Fig 7. Variation of moment M_e with uncracked depth

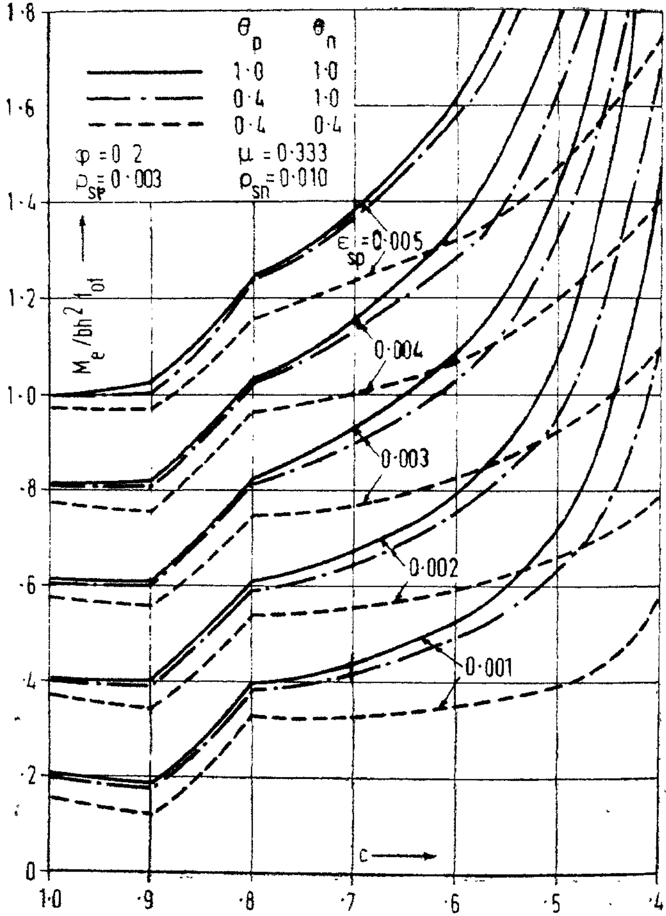

Fig. 8. Variation of movement (M_e) with uncracked depth-Influance of bond factor and effective prestrain.

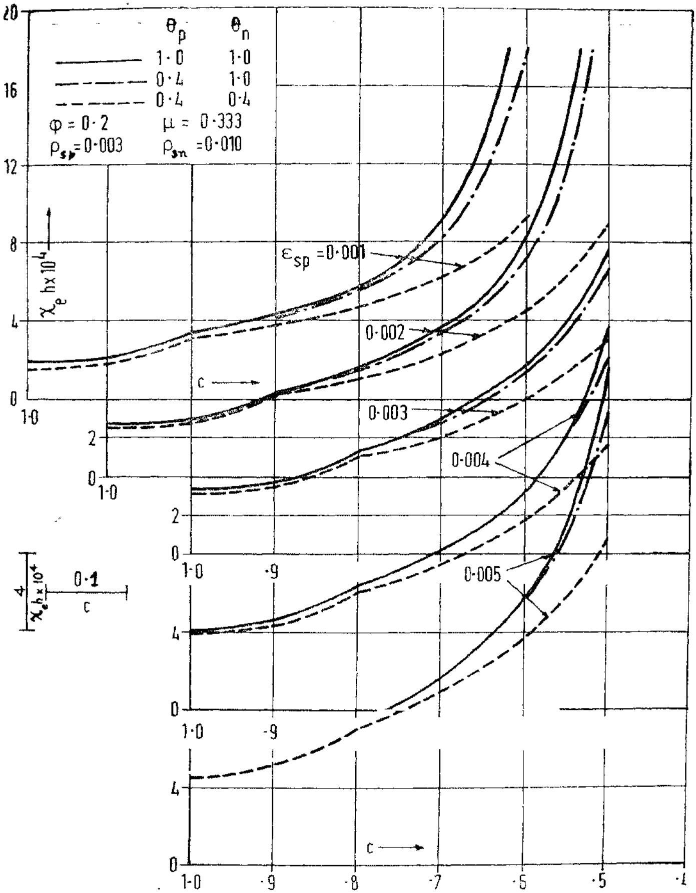

Fig. 9. Variation of curvature (χ_e) with uncracked depth-Influence of bond factor and effective prestrain.

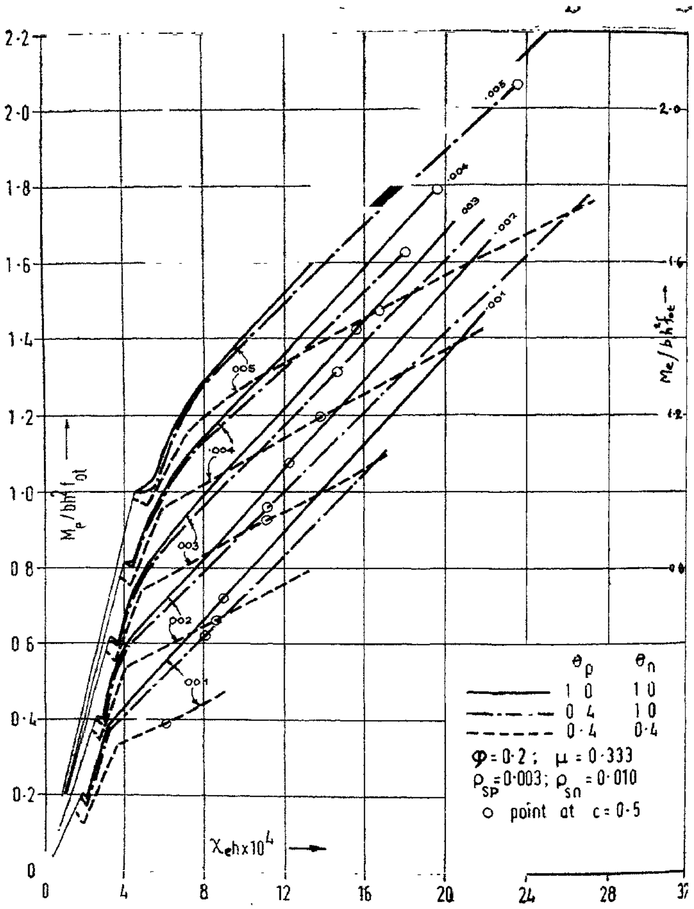

Fig. 10. Variation of moment with curvature after the inception of crack-Influence of bond factor and effective prestrain.

(*d*) *Minimum steel for crack stability* : Tables I and II summarize all the combinations of ρ_{sp}, ϵ_{sp} and ρ_{sn} for which the crack is found stable from the stage of inception, for the two sets of cross-sectional proportions examined.

For the combinations of prestressed and non-tensioned steel studied writing,

$$R = R_p + R_n \tag{30}$$

where

$$R_p = \frac{f_{su} A_{sp}}{f_{cu} bh (1 - r)} \tag{31 a}$$

and

$$R_n = \frac{f_{syn} A_{sn}}{f_{cu} bh (1 - r_n)} \tag{31 b}$$

the minimum value of R for a stable crack, say R_c, can be determined from the results in Tables I and II. Noting that higher values of ϵ_{sp} lead to smaller values of R_c, results in Table I have been examined for $\epsilon_{sp} = 0 \cdot 004$ and $0 \cdot 005$ and $\theta_p = \theta_n = 1 \cdot 0$ and the values of R_c determined for the stability of crack from its inception are given in Table III. It is possible that when the stability of a crack is taken as a criterion in the design, the cross-section, in some cases, may need much more steel than is required from strength considerations only. Under such circumstances, it may be desirable to permit a crack which is unstable only over a partial height and the stability of which is assured after in initial instability. A suitable design procedure could be to first design the steel required for the strength and then to check up for crack stability (with the hlep of tables such as Tables I and II) and if the latter is not satisfied, to introduce such alterations that ϵ_{sp}, ρ_{sp} and ρ_{sn} are adjusted as close as possible to a stable (or partly stable) crack combination without impairing the serviceability and strength requirements. Such an approach to class 3 prestressed beams could lead to designs which give a better postcracking performance.

TABLE I

Combinations of ρ_{sp}, ϵ_{sp} and ρ_{sn} for a stable crack for $\phi = 0{\cdot}2$ and $\mu = 0{\cdot}333$.

S No	ρ_{sp}	ϵ_{sp}	ρ_{sn}				
1	0 001	0 001	0	·005	·010	·015	·020
		0 002	0	·005	·010	·015	·020
		0 003	0	·005	·010	·015	·020
		0 004	0	·005	·010	·015	·020
		0 005	0	·005	·010	·015	·020
2	0 002	0 001	0	·005	·010	·015	·020
		0 002	0	·005	·010	·015	·020
		0 003	0	·005	·010	·015	·020
		0 004	0	·005	·010	·015	·020
		0 005	0	·005	·010	·015	·020
3	0 003	0 001	0	·005	·010	·015	·020
		0 002	0	·005	·010	·015	·020
		0 003	0	·005	·010	·015	·020
		0 004	0	·005	·010	·015	·020
		0 005	0	·005	·010	·015	·020
4	0 004	0 001	0	·005	·010	·015	·020
		0 002	0	·005	·010	·015	·020
		0 003	0	·005	·010	·015	·020
		0 004	0	·005	·010	·015	·020
		0 005	0	·005	·010	·015	·020
5	0 005	0 001	0	·005	·010	·015	·020
		0 002	0	·005	·010	·015	·020
		0 003	0	·005	·010	·015	·020
		0 004	0	·005	·010	·015	·020
		0 005	0	·005	·010	·015	·020

Cases for which crack is stable from its inception for $\theta_p = \theta_n = 1{\cdot}0$

-Do- -Do- -Do- for $\theta_p = 0{\cdot}4$, $\theta_n = 1{\cdot}0$

-Do- -Do- -Do- for $\theta_p = \theta_n = 0{\cdot}4$

TABLE II

Combination of ρ_{sp}, ϵ_{sp} *and* ρ_{sn} *for a stable crack for* $\phi = 0{\cdot}16$ and $\mu = 0{\cdot}20$

S No.	ρ_{sp}	ϵ_{sp}	ρ_{sn}				
1	0.001	0.001	0	·005	·010	·015	·020
		0.002	0	·005	·010	·015	·020
		0.003	0	·005	·010	·015	·020
		0.004	0	·005	·010	·015	·020
		0.005	0	·005	·010	·015	·020
2	0.002	0.001	0	·005	·010	·015	·020
		0.002	0	·005	·010	·015	·020
		0.003	0	·005	·010	·015	·020
		0.004	0	·005	·010	·015	·020
		0.005	0	·005	·010	·015	·020
3	0.003	0.001	0	·005	·010	·015	·020
		0.002	0	·005	·010	·015	·020
		0.003	0	·005	·010	·015	·020
		0.004	0	·005	·010	·015	·020
		0.005	0	·005	·010	·015	·020
4	0.004	0.001	0	·005	·010	·015	·020
		0.002	0	·005	·010	·015	·020
		0.003	0	·005	·010	·015	·020
		0.004	0	·005	·010	·015	·020
		0.005	0	·005	·010	·015	·020
5	0.005	0.001	0	·005	·010	·015	·020
		0.002	0	·005	·010	·015	·020
		0.003	0	·005	·010	·015	·020
		0.004	0	·005	·010	·015	·020
		0.005	0	·005	·010	·015	·020

Cases for which crack is stable from its inception for $\theta_p = \theta_n = 1.0$

-Do- -Do- -Do- for $\theta_p = 0.4$, $\theta_n = 1.0$

-Do- -Do- -Do- for $\theta_p = \theta_n = 0.4$

TABLE III

Minimum R-values R_c for crack stability for the case $\phi = 0 \cdot 2$, $\mu = 0 \cdot 33$ $\theta_p = \theta_n = 1 \cdot 0$

$\epsilon_{sp} = 0 \cdot 004$				$\epsilon_{sp} = 0 \cdot 005$			
ρ_{sp}	R_p	R_n	R_c	ρ_{sn}	R_p	R_n	R_c
0·002	0·0906	0·1710	0·2616	0·001	0·0453	0·2280	0·2733
0·003	0·1359	0·1140	0·2499	0·002	0·0906	0·1710	0·2616
0·004	0·1812	0·0570	0·2382	0·003	0·1359	0·1140	0·2499
0·005	0·2265	0·0570	0·2835	0·004	0·1812	0·0570	0·2382
				0·005	0·2265	0	0·2265

CONCLUSION

Stability of flexural cracks can be examined by using the proposed analysis. For a given data of material properties, sectional proportions and bonding efficiency, combinations of prestrain and areas of tensioned and non-tensioned steels which result in a crack which is stable either over the whole depth or over part-depth can be determined. Such data could be used in the design of class 3 prestressed concrete beams so that they have a better post-cracking performance.

ACKNOWLEDGEMENT

This paper forms a part of an investigation undertaken by the author at the University of Leeds during 1973–74. He is grateful to Prof. A. M. Neville and Dr. E. W. Bennett of the University of Leeds for their suggestions and for providing all the facilities for the research. He is also grateful to Prof. K. T. S. Iyengar and Prof. S. Dhawan of the Indian Institute of Science for deputing him for the research work. The author was supported by a Commonweatlth Academic Staff Fellowship during his stay in the United Kingdom.

Appendix I

Figure A1 showing the relation between cylinder strength and direct tensile strength.

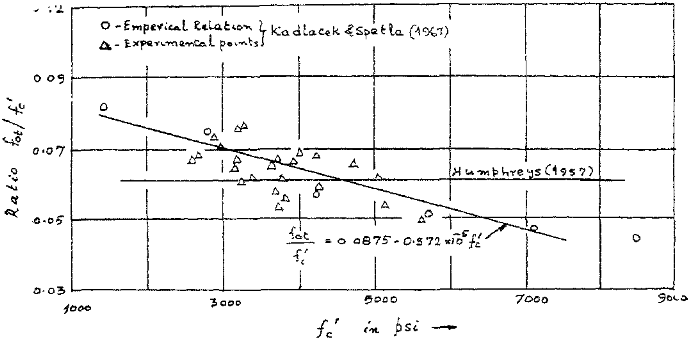

Fig. A1. Relation between Cylinder strength f_{et}/f_c.

Appendix II—Notation

A_{sp}	Area of prestressing steel;
A_{sn}	Area of non-tensioned steel;
b	Breadth of flange of I-section or breadth of a rectangular section;
C	Total compression;
C_f	Compression in concrete in top flange overhang;
C_w	Compression in web concrete;
c	Ratio of depth of uncracked section to overall depth;
E_c	Static secant modules of elasticity of concrete;
E_{s1}	Modulus of elasticity of prestress steel;
E_{s2}	Slope of the second line in the bilinear representation of the stress-strain curve of prestress steel;
E_{sn}	Modulus of elasticity of non-tensioned steel;
e	Base of Napierian logarithms;
f_c	Compressive stress in concrete;

$f'_c(=f_{oc})$ Cylinder compressive strength of concrete;

f_{cu} Cube compressive strength of concrete;

f_{ot} Tensile strength of concrete;

f_s Stress in prestress steel;

f_{sn} Stress in non-tensioned steel;

f_{sy} Stress at 0·2 per cent offset strain in prestress steel;

f_{syn} Yield strength of non-tensioned steel;

f_{su} Ultimate strength of prestress steel;

f_t Tensile stress in concrete

h Overall depth;

k Ratio of depth of neutral axis to overall depth;

M Bending moment;

M_{de} Moment at the decompression stage;

M_e Moment in excess of that at decompression stage $(=M - M_{de})$;

R Total reinforcement index;

R_c Minimum R-value for a stable crack;

R_n Non-tensioned steel index;

R_p Prestress steel index;

r_h Cover to centre of prestress steel;

r_{nh} Cover to centre of non-tensioned steel;

T Total tension in concrete;

T_f Tension in concrete in bottom flange overhang;

T_s Tension in prestress steel;

T_{sn} Tension in non-tensioned steel;

T_w Tension in concrete in the web;

y_{cf}	Distance of C_f from neutral axis;
y_{cw}	Distance of C_w from neutral axis;
y_{tf}	Distance of T_f from neutral axis;
y_{ts}	Distance of T_s from neutral axis;
y_{tsn}	Distance of T_{sn} from neutral axis;
y_{tw}	Distance of T_w from neutral axis;
α_c, α_{c12}	Factors giving average stress for compression in concrete;
α_t, α_{t12}	Factors giving average stress for tension in concrete;
β_c, β_{c12}	Factors giving distance to centroid of compression in concrete;
β_t, β_{t12}	Factors giving distance to controid of tension in concrete;
ϵ_c	Strain in concrete in compression;
ϵ_{c1}	Compressive strain in concrete at the bottom of the ecompression flange;
ϵ_{c2}	Extreme fibre strain of concrete in compression;
ϵ_{oc}	Compressive strain of concrete at f_{oc}
ϵ_s	Strain in steel;
ϵ_{ot}	Tensile strain of concrete at f_{ot};
ϵ_{sn}	Strain in A_{sn} at decompression stage;
ϵ'_{sn}	Strain in concrete at the level of A_{sn} due to moment M_e;
ϵ_{sp}	Effective prestrain, *i.e.*, strain in A_{sp} at the decompression stage;
ϵ'_{sp}	Strain in concrete at the level of A_{sp} due to moment M_e;
ϵ_{t1}	Tensile strain in concrete at the top of tension flange;
ϵ_{t2}	Limiting tensile strain in concrete (taken equal to ϵ_{ot});
ϵ_{sy}	Strain at the stress f_{sy} of the prestress steel;
ϵ_{syn}	Strain at yield stress of non-tensioned steel;

θ_p Bond factor of prestress steel;

θ_n Bond factor of non-tensioned steel;

μ Ratio of breadth of web to breadth of flange;

ρ_{sp} Ratio A_{sp}/bh;

ρ_{sn} Ratio A_{sn}/bh;

ϕ Ratio of thickness of flange to overall depth;

χ Curvature corresponding to moment M;

χ_e Curvature corresponding to moment M_e;

REFERENCES

[1] CEB-FIP Joint Committee — *International Recommendations for the Design and Construction of Concrete Structures*, Cement and Concrete Association, London 1970.,

[2] Krahl, N. W., Khachaturian N. and Siess, O. P. — Stability of tensile cracks in concrete beams. *Journal of the Structural Division*, American Society of Civil Engineers, 1967, **93** (St. 1), 23–254.

[3] Oladapo, I. O. .. Stability of tensile cracks in prestressed concrete beams, *Journal of the Structural Division*, American Society of Civil Engineers, 1969, **95** (St. 1), 17–31.

[4] Beeby, A. W. .. *An Investigation of Cracking in Slabs Spanning One Way*, Technical Report 42-433, 1970, Cement and Concrete Association, London.

[5] Beeby, A. W. .. *An Investigation of Cracking on the Side Faces of Beams*, Technical Report 42-466, 1971, Cement and Concrete Association, London.

[6] Desayi, P. .. *Some Studies on the Flexural Cracking of Partially Prestressed Concrete Beams*, Research Report, 1974, Civil Engineering Department, University of Leeds, Leeds.

[7] Desayi, P. and Krishnan. S. — Equation for stress-strain curve of concrete, *Journal of the American Concrete Institute*, 1964, **61** (3), 345–350. Discussions, *61* (9), 1229–1235.

[8] Humphreys, R. .. Direct tensile strength of concrete, *Civil Engineering and Public Works Review*, 1957, **52** (614), 882–884.

[9] Kadlacek, V. and Spetla, I. — Direct tensile strength of concrete, *Journal of Materials* American Society of Testing and Materials, 1967, **2** (4) 749–767.

[10] Todd, J. D. .. The determination of tensile stress-strain curves of concrete *Proceedings*, Institution of Civil Engineers (London), 1955, 4, (2, Part I), 201–211.

[11] Evans, R. H. .. Microcracking and stress-strain curves for concrete in tension, *Materials and Structures, Research and Testing (RILEM,)*, 1968, **1** (1), 61–64.

[12] Bennett, E. W. and O'Keeffe, J. D. The influence of bond on the flexural strength of prestressed concrete beams, Parts I, II and III. *Civil Engineering and Public Works Review*, 1958, **53** (630), 1391–1393; 1959, **54** (631), 88–90 and **54** (632), 209–212.